

# The Impact of Pedestrian Lane Formation by Obstacles on Fire Evacuation Efficiency in the Presence of Unfair Competition

Shanwei Liu, Xiao Li, Bozhezi Peng and Chaoyang Li \*

School of Ocean and Civil Engineering, Shanghai Jiao Tong University, Shanghai 200240, China; themanfromearth@sjtu.edu.cn (S.L.); li\_xiao@sjtu.edu.cn (X.L.); bozhezi.peng@sjtu.edu.cn (B.P.)

\* Correspondence: cyljif@sjtu.edu.cn

**Abstract:** After a fire breaks out, pedestrians simultaneously move towards the exit and quickly form a crowded area near the exit. With the intensification of pedestrians' tendencies towards unfair competition, there is an increase in pushing and collisions within the crowd. The possibility of stampedes within the crowd also gradually increases. Analyzing the causes and psychological tendencies behind pedestrian pushing and collisions has a positive effect on reducing crowd instability and improving evacuation efficiency. This research proposes a modified social force model considering the unfair competition tendency of pedestrians. The model considers factors such as the gap between pedestrians' actual and maximum achievable speed, effective radius, and their distance from the exit. In order to overcome the shortage of "deadlock" in the classical social force model in a high-density environment, this research introduces the feature of variable pedestrian effective radius. The effective radius of pedestrians dynamically changes according to the density of the surrounding crowd and queuing time. Through validation, the evacuation efficiency of this model aligns well with the actual situation and effectively reflects pedestrians' pushing and squeezing behaviors in high-density environments. This research also analyzes how to strategically arrange obstacles to mitigate the exacerbating effect of unfair pedestrian competition on exit congestion. Five experiments were conducted to analyze how the relative position of obstacles and exits, the number of evacuation paths, and the size of the obstacle-free area before the exit affect evacuation efficiency in the presence of unfair pedestrian competition. The results show that evacuation efficiency can be improved when obstacles play a role in guiding or reducing the interaction of pedestrians in different queues. However, when obstacles hinder pedestrians, the evacuation efficiency is reduced to a certain extent.

**Keywords:** crowd evacuation; crowded exit; unfair competition; effective radius; social force model

**Citation:** Liu, S.; Li, X.; Peng, B.; Li, C. The Impact of Pedestrian Lane Formation by Obstacles on Fire Evacuation Efficiency in the Presence of Unfair Competition. *Fire* **2024**, *7*, 242. <https://doi.org/10.3390/fire7070242>

Academic Editor: Jianping Zhang

Received: 4 June 2024

Revised: 3 July 2024

Accepted: 8 July 2024

Published: 10 July 2024



**Copyright:** © 2024 by the authors. Licensee MDPI, Basel, Switzerland. This article is an open access article distributed under the terms and conditions of the Creative Commons Attribution (CC BY) license (<https://creativecommons.org/licenses/by/4.0/>).

## 1. Introduction

In recent years, pedestrian dynamics and crowd evacuation have received increasing attention, which has significant practical implications for understanding pedestrian movement after a fire and improving evacuation efficiency [1]. Social force model is one of the most commonly used methods for simulating pedestrian movement [2,3]. Many observed pedestrian collective dynamic behaviors have been successfully described by social force model, as shown in Table 1.

After a fire, a large number of pedestrians simultaneously move towards the exit, leading to the rapid formation of a high-density area near the exit. High density alters pedestrian behavior [4], leading to increased crowd flow and unstable movement [5]. This appears to be the most complex area [6]. In a high-density environment, pedestrians may push and collide [7], which can escalate into a severe stampede accident [8]. Analyzing and understanding the causes of pushing and collisions among pedestrians is essential for reducing stampede accidents and enhancing public safety. Pushing and collisions are

caused by pedestrians' desire to compete for target space through unfair competition [9,10]. Whether pedestrians engage in unfair competition behavior directly depends on the gap between their actual walking speed and their maximum achievable speed. When pedestrians' actual walking speed is close to their maximum achievable speed, the possibility of unfair competition behavior remains at a low level. However, as the actual walking speed of pedestrians decreases, the possibility of unfair competition behavior will increase [11,12]. Crowd density is an important factor influencing the occurrence of unfair competition behavior [13]. The possibility of unfair competition among pedestrians is positively correlated with crowd density and increases as crowd density increases [14]. Additionally, the tendency for pedestrians to engage in unfair competition is also affected by the distance between pedestrians and the exit [15]. The number of people discontent with waiting in line increases with the distance from the exit [16]. The desired speed, as one of the parameters in the social force model, is a crucial factor influencing the model's performance [17–19]. When pedestrians engage in pushing behavior, their desired speed undergoes changes, leading pedestrians to acquire higher desired speed [20,21]. A higher desired speed produces more collisions, and the real manifestation of such collisions is pushing and shoving. This research introduces unfair competition into the social force model. Through the unfair competition factor, pedestrians achieve higher desired speed, resulting in more collisions. This factor is influenced by the gap between pedestrians' actual and maximum achievable speed, queue distance, and other factors.

The pathway opened by pushing is relatively narrow, making it difficult for pedestrians to pass through in a conventional manner. However, pedestrians are highly adaptable in their movements and employ various methods to navigate through [22]. In narrow spaces, pedestrians can pass through crowds by actively rotating or contracting their bodies [23,24]. The classical social force model typically sets the contact or force distance of pedestrians to a fixed value. Pedestrians are represented as circles during the simulation process. However, the fixed-size circular model often results in deadlock in narrow spaces [25]. Simply treating pedestrians as circles neglects the body movements of pedestrians in narrow spaces [26]. The elliptical social force model can partially address this issue, but the calculation of the minimum distance for ellipses is complex [27]. Existing research on elliptical social force model mainly calculates the repulsion between pedestrians by determining the distance between their centers of mass [28–31]. However, the shortest distance between two ellipses does not necessarily occur along the line connecting their centers of mass. This simplification may lead to discrepancies between simulation results and the actual bodily rotational or contraction behaviors of pedestrians. The essence of rotating or contracting the body is to adjust the effective radius of pedestrians to fit the width of narrow spaces. Representing pedestrians as size-variable circles not only reflects the adjustment of pedestrians' effective radius but also avoids complex geometric calculations [32]. In order to enhance the navigability of the classical social force model in high-density areas, this research introduces the feature of the variable pedestrian effective radius, which dynamically adjusts the pedestrian's effective radius based on external conditions.

When people face the efforts they have exerted, they often tend to persist with the decisions they have made. This phenomenon is known as the sunk cost effect [33,34]. Pedestrians need to rotate or contract their bodies when squeezing through gaps in a crowd, which requires additional efforts. Those efforts somewhat predispose pedestrians to continue engaging in unfair competition behaviors. In other words, in order to achieve rapid passage through an exit, pedestrians' unfair competition behavior demands more body movements. More body movements, to a certain extent, sustain the tendency of unfair competition. Therefore, this research also considers the impact of changes in pedestrian body size on the tendency towards unfair competition.

For indoor environments, the formation of evacuation paths is influenced by the layout of obstacles [35]. Ref. [36] provides the minimum net width value of evacuation walkways. That is, it stipulates the minimum distance between the obstacles on both sides of the evacuation path. However, there are no clear requirements for the number of

evacuation paths, the relative position relationship between evacuation paths and room evacuation doors, or the distance between obstacles and room evacuation doors. The reasonable layout of obstacles can improve the outlet flow velocity and significantly reduce the probability of congestion [37]. In this study, a cylindrical obstacle was set up near the exit to divide a crowd. In real life, the space in the room is relatively limited, making it challenging to place an obstacle near the exit. Further analysis is needed on how to divide and guide a crowd by utilizing the conventional and existing obstacles in the room. The exit layout constitutes another crucial factor affecting crowd evacuation [38]. However, the study did not address obstacles, and all pedestrians were in free motion. For rooms with obstacles, pedestrian movement is restricted. Further discussion is needed on the relative positioning of obstacles and exits. The impact of obstacles on exit evacuation efficiency is constrained by their distance [39]. However, this study only discusses scenarios where pedestrians do not engage in unfair competition. In high-density environments, pushing and collisions among pedestrians are significant causes of crowd instability. It is necessary to analyze the impact of obstacles on exit evacuation efficiency when there is unfair competition among pedestrians.

This research analyzes the motion characteristics of pedestrian pushing and squeezing through gaps in crowd behaviors and proposes a modified social force model that considers pedestrians’ unfair competition and variable body size. This research provides the formula for calculating the desired speed of pedestrians during pushing, as well as the variation of pedestrian radius during the process of squeezing through gaps in the crowd. The simulation results demonstrate that the model effectively captures the unfair competition and squeezing behaviors of pedestrians near a crowded exit after a fire occurs. In order to mitigate the exacerbating effect of unfair competition on exit congestion, this research analyzes the intrinsic principles of how obstacle layout affects evacuation efficiency through experiments. It concludes that evacuation efficiency can be improved when obstacles play a role in guiding or reducing the interaction of pedestrians in different queues.

**Table 1.** Research on the social force model.

Pedestrian Behavior	References	Pros and Cons
Faster is slower	Helbing et al. [20]	<ul style="list-style-type: none"> <li>• By introducing pedestrian emotion, pedestrians are given a higher desired speed. The simulation demonstrates that the average departure speed of groups of pedestrians decreases with the increase in the desired speed of individual pedestrians.</li> <li>• Although the model considers the gap between pedestrians’ actual and maximum achievable speed, it does not account for the influence of factors such as crowd density, queue time, queue distance, and others on pedestrian emotions.</li> </ul>
Stop-and-go	Yu et al. [40]	<ul style="list-style-type: none"> <li>• A new repulsive force is added to the model, enabling the classical social force model to better replicate local interactions in regions of extreme density. The simulation results demonstrate the transition of pedestrians from laminar flow to stop-and-go and turbulence.</li> <li>• The model better reflects the movement characteristics of pedestrian groups, but it</li> </ul>

		ignores the body movements and heterogeneity of individual pedestrians.
Bidirectional pedestrian flow stratification	Helbing et al. [41]	<ul style="list-style-type: none"> <li>The study provides a new perspective on understanding the phase transition behavior of systems far from equilibrium, emphasizing the crucial role of fluctuations in promoting or disrupting the formation of ordered structures.</li> <li>However, the simulation environment is relatively simple, without considering the impact of obstacles on pedestrians along their forward path. Obstacles are also important factors affecting pedestrian flow patterns.</li> </ul>
Overtaking	Yuen et al. [42]	<ul style="list-style-type: none"> <li>The study introduces visual factors based on the classical social force model. Pedestrians adjust their motion state according to the state of other pedestrians within a certain range. The model achieves overtaking behavior while minimizing unrealistic collisions.</li> <li>The study only considers pedestrians overtaking by adjusting their direction of movement. It overlooks the behavior where pedestrians can squeeze through the gaps in the crowd by rotating or contracting their bodies.</li> </ul>

## 2. Model Description

### 2.1. Classical Social Force Model (SFM)

The classical social force model suggests that pedestrian movement is influenced by both intrinsic and extrinsic social force [43]. Internal social force reflects the driving force of individual subjective consciousness. Extrinsic social forces include the forces between pedestrians and the forces between pedestrians and boundaries or obstacles. The resultant force is shown in Equation (1).

$$\vec{f}_i(t) = \vec{f}_i^0 + \sum_{j(\neq i)} \vec{f}_{ij} + \sum_w \vec{f}_{iw} \tag{1}$$

where  $\vec{f}_i(t)$  represents the resultant force acting on pedestrians,  $\vec{f}_i^0$  represents the driving force,  $\sum_{j(\neq i)} \vec{f}_{ij}$  represents the repulsive force between pedestrians, and  $\sum_w \vec{f}_{iw}$  represents the repulsive force of boundaries or obstacles on pedestrians.

The driving force of pedestrians is shown in Equation (2).

$$\vec{f}_i^0 = \frac{m_i \cdot (v_i^0(t) \cdot \vec{e}_i^0 - \vec{v}_i(t))}{\tau_i} \tag{2}$$

where  $m_i$  represents the mass of pedestrians,  $v_i^0(t)$  represents the desired speed of pedestrians in the direction  $\vec{e}_i^0$ ,  $\vec{v}_i(t)$  represents the actual velocity of pedestrians at time  $t$ , and  $\tau_i$  represents the response time of pedestrians to adjust their speed and direction.

The repulsive force between pedestrians is shown in Equation (3).

$$\vec{f}_{ij} = \left\{ A_i \exp\left[\left(r_{ij} - d_{ij}\right) / B_i\right] + kg\left(r_{ij} - d_{ij}\right)\right\} \vec{n}_{ij} + \kappa g\left(r_{ij} - d_{ij}\right) \Delta \vec{v}_{ij}(t) \vec{t}_{ij} \quad (3)$$

where  $A_i$  represents the strength of interaction force between pedestrians  $i$  and  $j$ ;  $B_i$  represents the range of interaction force between pedestrians  $i$  and  $j$ ;  $k$  and  $\kappa$  are constants; Function  $g(x)$  is a conditional function, which is zero if pedestrians do not contact each other, otherwise it equals the parameter  $x$ ;  $r_{ij}$  represents the sum of the radius of pedestrian  $i$  and  $j$ ;  $d_{ij}$  represents the shortest distance between pedestrian  $i$  and  $j$ ;  $\vec{n}_{ij}$  represents the unit vector pointing from pedestrian  $i$  to  $j$ ; and  $\Delta \vec{v}_{ij}(t) = \left(\vec{v}_j(t) - \vec{v}_i(t)\right) \cdot \vec{t}_{ij}$  represents the velocity difference between pedestrians  $i$  and  $j$  in the tangential direction.

The repulsive force between pedestrians and obstacles is shown in Equation (4).

$$\vec{f}_{iw} = \left\{ A_i \exp\left[\left(r_i - d_{iw}\right) / B_i\right] + kg\left(r_i - d_{iw}\right)\right\} \vec{n}_{iw} + \kappa g\left(r_i - d_{iw}\right) \left(\Delta \vec{v}_i(t) \cdot \vec{t}_{iw}\right) \vec{t}_{iw} \quad (4)$$

where  $d_{iw}$  represents the shortest distance between pedestrian  $i$  and obstacle  $W$ ,  $\vec{n}_{iw}$  represents the direction perpendicular to pedestrian  $i$  and obstacle  $W$ , and  $\vec{t}_{iw}$  represents the tangential direction between pedestrian  $i$  and obstacle  $W$ .

### 2.2. Modified Social Force Model (MSFM)

The MSFM extends the rules of describing pedestrian movement from the SFM, analyzing behaviors of pushing and squeezing through gaps in the crowd from both psychological and physiological aspects. It overcomes the shortcomings of the SFM in describing pedestrian unfair competition and bodily details.

The pushing among pedestrians arises from highly competitive or even aggressive behavior [44,45]. The schematic diagram of pedestrians pushing is shown in Figure 1a. The unfair competition tendencies among pedestrians are controlled by the actual walking speed and the maximum achievable speed. When pedestrians' actual walking speed is lower than the maximum achievable speed, the possibility of pushing behavior among pedestrians tends to increase [12,46]. This tendency is also positively correlated with the distance between pedestrians and the exit. As the queue lengthens, pedestrians become impatient, and the number of pedestrians choosing to conservatively continue queuing decreases [47]. After pushing, pedestrians need to rotate or contract their bodies to successfully navigate through dense crowds. This process requires more effort than adhering to a conservative queuing strategy. Based on the sunk cost effect, pedestrians who exert more effort tend to persist with their decisions [33,34]. To some extent, the behavior of pedestrians of adjusting body posture upholds the tendency of unfair competition. For the social force model, assigning a higher desired speed to pedestrians can result in more collisions. Based on the above research, we present a factor reflecting the unfair competition tendency of pedestrians, enabling pedestrians to achieve higher desired speed. This factor considers factors such as the gap between pedestrians' actual and maximum achievable speed, pedestrian effective radius, and distance to the exit, as shown in Equation (5).

$$\omega_i(t) = \left(1 - \frac{\vec{v}_i(t)}{\vec{v}_i^{\max}}\right) \cdot \exp\left\{-1 - \alpha \cdot \left[\left(\frac{r_i(t) - b_i}{a_i - b_i}\right) \cdot d\right]\right\} \quad (5)$$

where  $\omega_i(t)$  represents the unfair competition factor;  $\vec{v}_i^{\max}$  represents the maximum achievable speed of pedestrians;  $\alpha$  is a sensitive parameter that controls the rate of

unfair competition tendency, which gradually decreases with the increase in  $\alpha$  value and reaches the maximum when  $\alpha = 0$ ;  $r_i(t)$  represents the effective radius of pedestrians;  $a_i$  represents the semi-major axis of pedestrians;  $b_i$  represents the semi-minor axis of pedestrians; and  $d$  represents the distance of pedestrians to the exit.

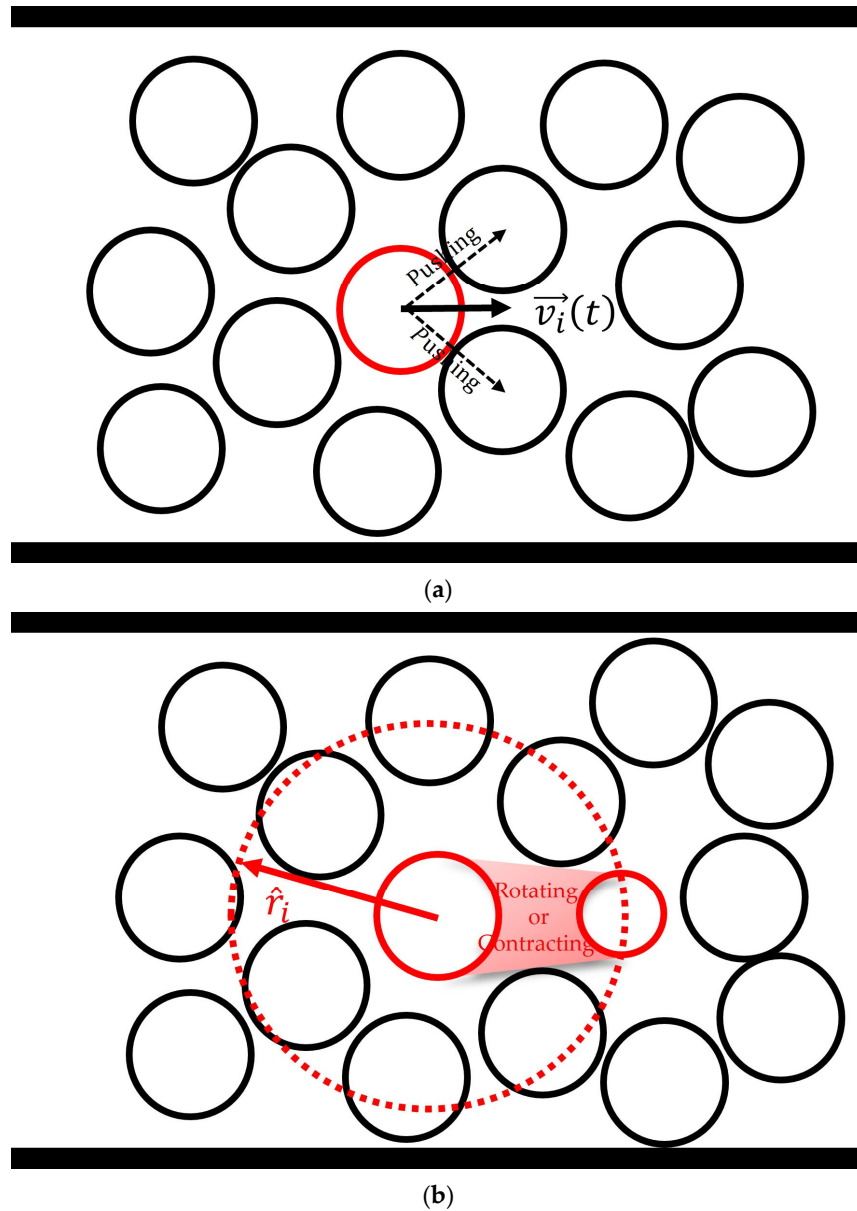


**Figure 1.** (a) Pedestrians compete for the target space by pushing, (b) pedestrians squeezing through gaps in the crowd by rotating or contracting their bodies.

The corrected desired speed of pedestrians  $v_i(t)$  is shown in Equation (6).

$$v_i(t) = \omega_i(t) \cdot v_i^0(t) + (1 - \omega_i(t)) \cdot v_i^{\max} \tag{6}$$

The SFM cannot enable pedestrians to pass through passages narrower than their diameter. The pathway opened by pushing is often narrow. A mechanism needs to be proposed to solve this problem. Pedestrians can change their personal space by rotating

or contracting their bodies. The purpose of these behaviors is to form a body with a smaller effective size, meaning that the size of pedestrians is variable [23]. Ref. [32] proposes a social force model that dynamically adjusts the pedestrian radius by perceiving gaps. However, the prerequisite is that an object can be found on both sides of the forward direction. If not, an assumption needs to be made. Perceiving gaps is essentially judged by visual information, but pedestrian motion decisions integrate a variety of sensory information. Pedestrians can not only observe other pedestrians through vision but also perceive those on the side or even behind through hearing and touch. This research proposes a strategy for pedestrians to adjust their body posture by sensing the occupation of space by other pedestrians within a certain range. This strategy reduces the requirement to find or assume gap boundaries. In this research, the perception range is set as a circle, and the key is to determine the radius of the perception circle. The schematic diagram of pedestrian perception is shown in Figure 1b. Queuing time also can influence pedestrian walking characteristics [48]. This research proposes a radius conversion factor, where pedestrians dynamically adjust their radius size by perceiving crowd density and queuing time. The radius conversion factor  $\psi_i(t)$  is shown in Equation (7).

$$\psi_i(t) = \frac{1}{1 + \exp\left[-\beta \cdot \left(\frac{\rho_{\max} - \rho}{\rho_{\max}} \cdot t\right)^{\frac{1}{\beta}}\right]} \tag{7}$$

where  $\rho_{\max}$  represents the maximum density that pedestrians can tolerate;  $\rho$  denotes the crowd density within the perception range, as shown in Equation (8); and  $\beta$  is a parameter adjusting the sensitivity and slope of the radius conversion factor.

$$\rho = \frac{N_p}{\pi \hat{r}_i^2} \tag{8}$$

where  $N_p$  represents the number of people within the perception range, and  $\hat{r}_i$  denotes the radius of the perception range, which is an integer multiple of the pedestrian's semi-major axis,  $\hat{r}_i = \lambda a_i$ .

The effective radius of pedestrians is shown in Equation (9).

$$r_i(t) = \psi_i(t) \cdot a_i + (1 - \psi_i(t)) \cdot b_i \tag{9}$$

### 3. Experimental Data and Parameter Values

The experimental data were obtained from an interdisciplinary experimental study on congestion and queuing in front of entrances conducted at the University of Wuppertal, and the video data with the identifier 030\_c\_56\_h0 were selected for analysis [49]. The experiment involved 75 volunteers whose initial positions were randomly distributed in a corridor measuring 7 m in length and 5.6 m in width. After the start of the experiment, volunteers were asked to pass through a bottleneck area with a width of 0.5 m as quickly as possible. The width of the exit allowed only one pedestrian to pass at a time.

This research focused on the behavior of pedestrians rotating or contracting their bodies in high-density environments, as illustrated in Figure 2. Supplementary analysis was conducted on 14 cases of pedestrians who were clearly observed performing the above-mentioned actions in the video. Statistics were gathered on factors such as the number of people surrounding these pedestrians and the rotation angle.



**Figure 2.** Pedestrians marked with blue circles navigate high-density areas by (a) rotating their bodies and (b) contracting their bodies.

Using the SFM to simulate the above data, it was found that when the exit width was less than 1 m, pedestrians could not be effectively evacuated. This is because in high-density environments, the combined effects of pedestrian repulsion and obstacle repulsion result in a phenomenon known as deadlock in pedestrian movement. Simply put, pedestrians become stuck between other pedestrians or obstacles. The simulation manifested as pedestrians being completely unable to move or oscillating within a certain range. Figure 3 reflects the variation of pedestrian distance to the exit over time with an exit width of 0.6 m. After 18 s of simulation, all pedestrians were unable to move. Figure 4a depicts the positions of all pedestrians after 45 s of simulation with an exit width of 0.8 m. Pedestrians 20 and 61 repeatedly collided. Pedestrian 61 became stuck between pedestrian 20 and the wall, unable to proceed further into the exit. The variation over time in the distance from pedestrians 20 and 61 to the exit is shown in Figure 4b.

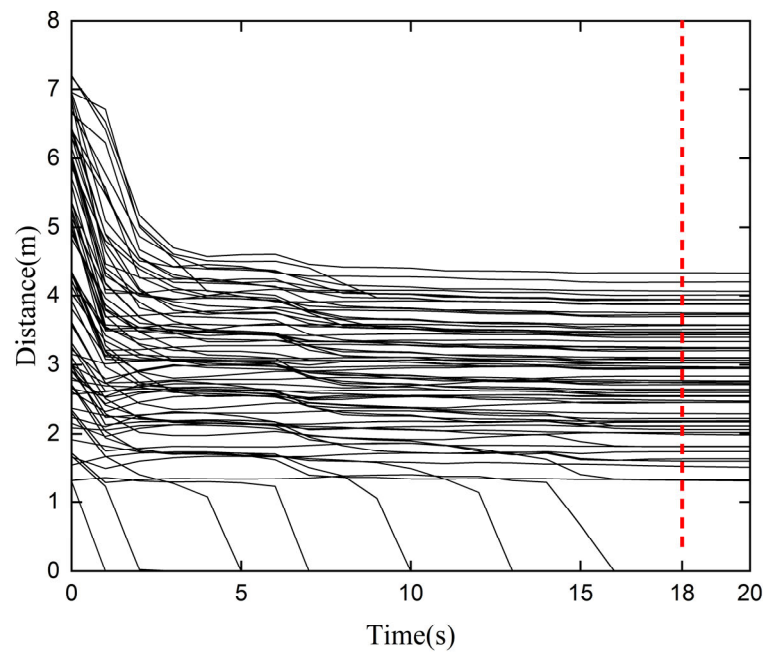


**Figure 3.** The variation in pedestrian distance to the exit over time with an exit width of 0.6 m. The red dotted line marks the distance of each pedestrian from the exit after 18 s of simulation.

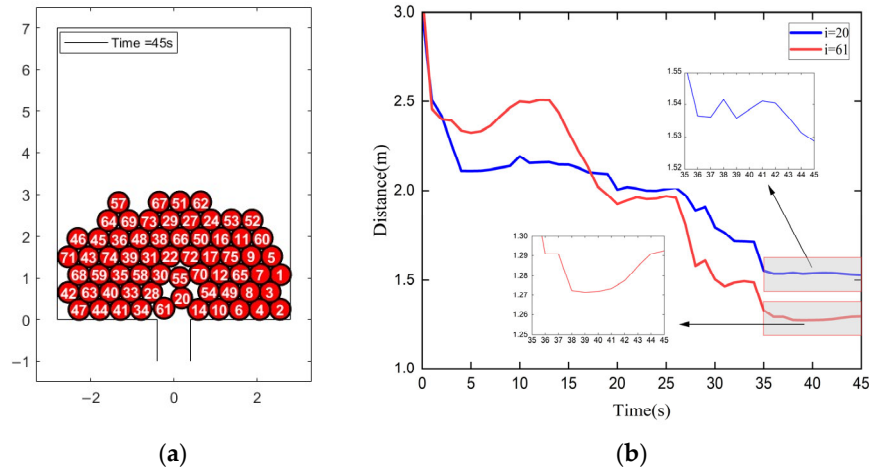


**Figure 4.** The simulation runs for 45 s with an exit width of 0.8 m. (a) The positions of all pedestrians, and (b) the variation over time in the distance from pedestrian 20 and pedestrian 61 to the exit.

After repeated testing, the exit width in the SFM was set to 1 m, allowing pedestrians to be effectively evacuated. Although the exit width did not match reality, pedestrians still could not pass side by side due to repulsion forces. The pedestrian number and coordinate system adopt the rules of Ref. [49].

The remaining parameters for pedestrians are listed in Table 2.

**Table 2.** The values of pedestrian parameters.

Parameters	Value
$m_i$	80 kg
$v_i^0(t)$	3 m/s
$\tau_i$	0.5 s
$A_i$	2000
$B_i$	0.08
$k$	$1.2 \times 10^5$
$\mathcal{K}$	$2.4 \times 10^5$
$\vec{v}_i^{\max}$	5 m/s
$r_i$	0.25 m
$a_i$	0.25 m
$b_i$	0.2 m
$\rho_{\max}$	9 ped/m <sup>2</sup> [45]

#### 4. Results

The number of pedestrians surrounding the 14 cases of pedestrians with body rotation or contraction movements clearly observed in the video was statistically analyzed using search radii of three, four, and five times the semi-major axis of the pedestrian. The results are shown in Figure 5. The standard deviation of the three groups of data is shown in Table 3. When the search radius was set at three times the semi-major axis of the pedestrian, the dispersion of the number of surrounding pedestrians was minimized. This indicates that the number of surrounding pedestrians was relatively stable within this range. At the same time, there was a possibility of direct contact among surrounding pedestrians within this range. Therefore, using this range as the perceptual range of pedestrians also aligns with general cognition.

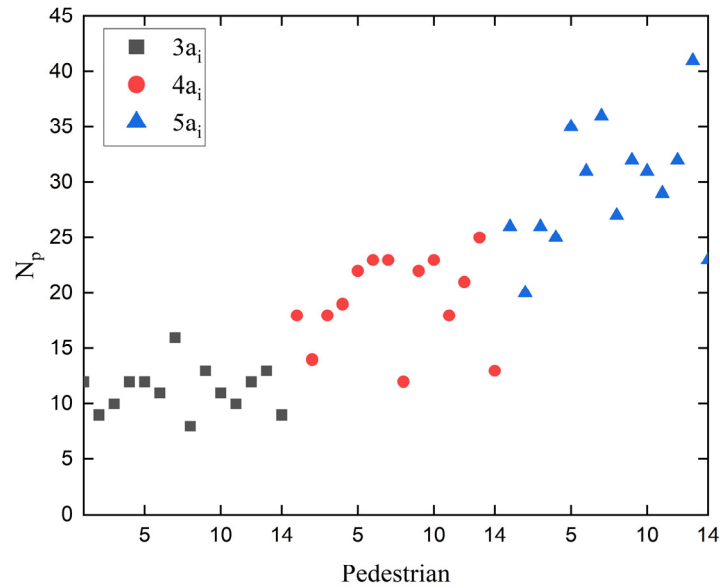


Figure 5. Statistics of the number of pedestrians around.

Table 3. Standard deviation of the number of surrounding pedestrians under different search radii.

Search Radius	$3a_i$	$4a_i$	$5a_i$
Standard deviation	2.01	4.03	5.92

To determine the value of  $\beta$ , this research conducted multiple numerical experiments and compared them with actual data, as shown in Appendix A. The mean absolute error between the results of each set of numerical experiments and actual data are shown in Table 4. The optimal fit value for  $\beta$  in this case was 0.75.

Table 4. The mean absolute error between the results of each set of numerical experiments and actual data for different  $\beta$ .

$\beta$	0.25	0.5	0.75	1
Mean absolute error	0.007479	0.007464	0.007421	0.007621

When the radius of the pedestrians was made variable, it was found that pedestrians could pass side by side through the exit when the exit width was set to 1 m. Therefore, the exit width needed to be adjusted. When the exit width was adjusted to 0.9 m, the phenomenon of pedestrians passing side by side disappeared. Therefore, in the MSFM, the exit width was adjusted to 0.9 m.

In the numerical experiments to determine  $\alpha$ , the number of evacuees was counted every 5 s and compared with actual data. Figure 6 shows the relationship between the number of evacuees and the time for different  $\alpha$ . The mean absolute error between the simulation results and actual data for different  $\alpha$  are shown in Table 5. The optimal fit value for  $\alpha$  in this case was 0.6.

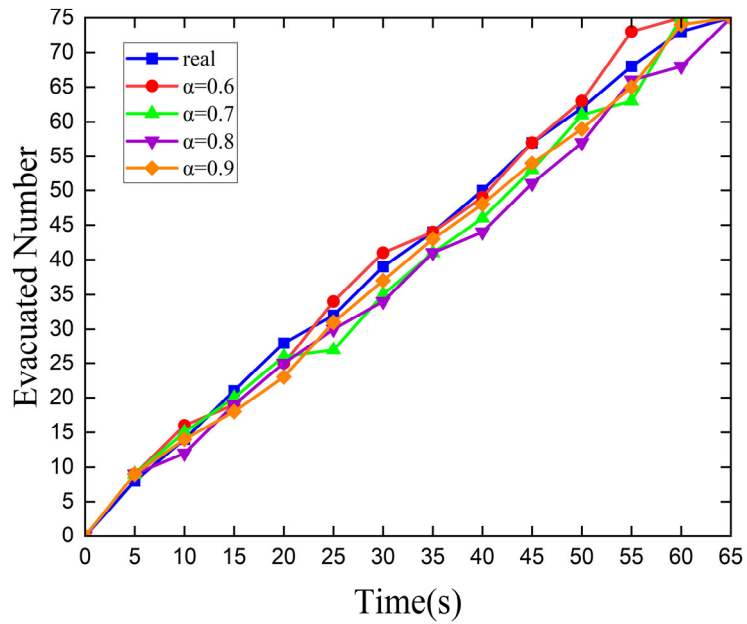


Figure 6. The relationship between the number of evacuees and time for different  $\alpha$  values.

Table 5. The mean absolute error between simulation results and actual data for different  $\alpha$  values.

$\alpha$	0.6	0.7	0.8	0.9
Mean absolute error	1.5	2.4	3	1.8

This research compared the number of evacuees over time between the MSFM and the SFM with different desired speeds. As shown in Figure 7, the MSFM could better estimate the macroscopic evacuation efficiency. The SFM, with an exit width of 1 m and desired speeds of 3 m/s, 4 m/s, and 5 m/s, failed to achieve complete evacuation within 65 s.

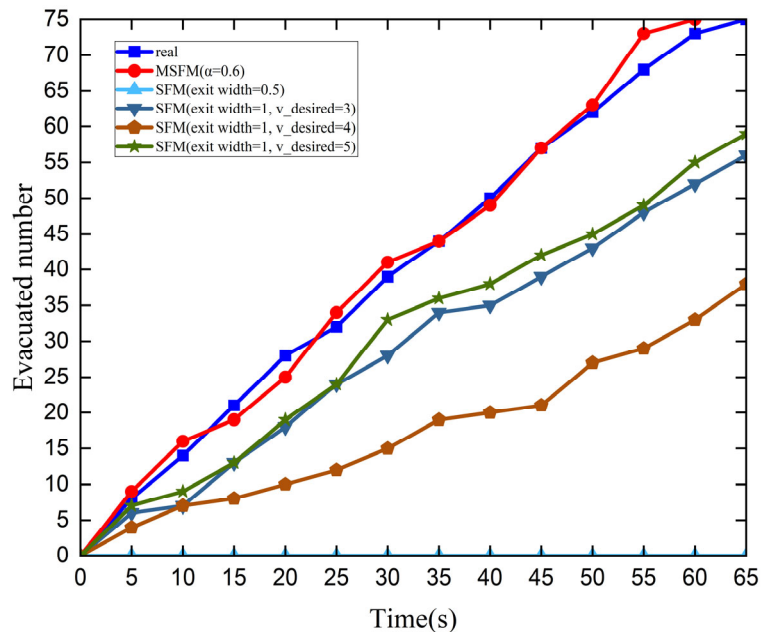


Figure 7. The variation in the number of evacuees over time.

### 5. Discussion

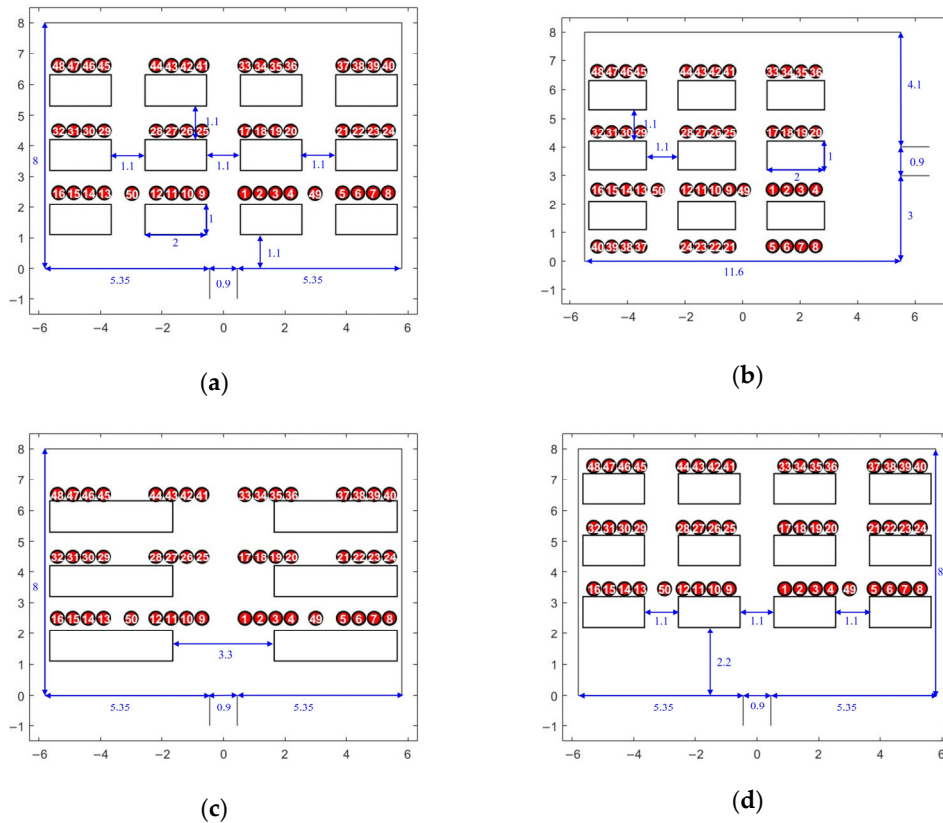
#### 5.1. Influence of Desired Speed on Evacuation Efficiency

Figure 7 shows that there was no significant difference in evacuation efficiency between  $v_{desired} = 3$  m/s and  $v_{desired} = 5$  m/s, but both were higher than  $v_{desired} = 4$  m/s. The authors believe that the reason for this is the coexistence of two seemingly contradictory phenomena: “faster is slower” [20] and “faster is faster” [50].

In this research, when  $v_{desired}$  increased from 3 m/s to 4 m/s, evacuation efficiency decreased, illustrating “faster is slower.” Pedestrians can move faster towards the exit after increasing their desired speed. However, pedestrians arriving earlier at the exit are not effectively evacuated, leading to continuous congestion near the exit and a reduction in evacuation efficiency. But with further increases in desired speed, pedestrians who arrive first quickly pass through the exit without significant accumulation. At this time, evacuation efficiency improves at this point, reflecting “faster is faster.” However, overall, despite increasing the desired speed from 3 m/s to 5 m/s, pedestrians exert more effort but evacuation efficiency does not improve.

#### 5.2. Influence of Obstacles on Evacuation Efficiency

To further analyze the influence of pedestrians’ unfair competition near crowded exits on emergency evacuation after a fire, this research conducted evacuation simulations with different layouts of obstacles, as shown in Figure 8. The simulation environment was  $11.6 \text{ m} \times 8 \text{ m}$ , with an exit width of 0.9 m.

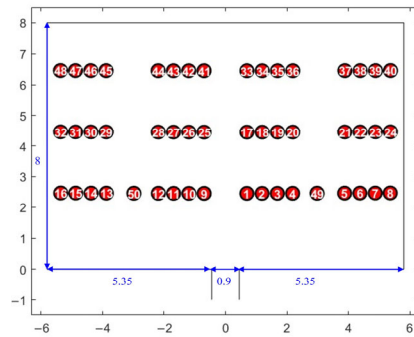


(a)

(b)

(c)

(d)



(e)

**Figure 8.** Layout of obstacles for each experiment: (a) Experiment 1, (b) Experiment 2, (c) Experiment 3, (d) Experiment 4, (e) Experiment 5.

In Experiment 1, obstacles measuring  $2\text{ m} \times 1\text{ m}$  were placed, totaling twelve. Pedestrians were evenly distributed behind the obstacles. According to Ref. [36], the minimum net width of evacuation walkways is  $1.1\text{ m}$ . Therefore, the lateral and longitudinal distances between obstacles, as well as the distance of the lowest row of obstacles from the bottom boundary, were all set to  $1.1\text{ m}$ .

Experiment 2 adjusted the exit to the right side of the overall layout, allowing pedestrians to move horizontally towards the exit. The purpose of this experiment was to analyze the impact of the relative position relationship between obstacles and the exit on pedestrian evacuation in unfair competition.

Experiment 3 combined the three  $1.1\text{ m}$  paths from Experiment 1 into a single  $3.3\text{ m}$  path. The purpose of this experiment was to analyze the impact of the number of paths on pedestrian evacuation in unfair competition.

In Experiment 4, obstacles were increased by  $1.1\text{ m}$  away from the exit based on the layout of Experiment 1. The purpose of this experiment was to analyze the influence of the size of the obstacle-free area in front of the exit on the evacuation of pedestrians in unfair competition.

Experiment 5 served as a control group without obstacles.

The relationships between the number of evacuees and time for the five experiments are shown in Figure 9. Evacuation counts were recorded every  $5\text{ s}$ . The evacuation times for each experimental group were  $35\text{ s}$ ,  $30\text{ s}$ ,  $50\text{ s}$ ,  $40\text{ s}$ , and  $55\text{ s}$ . Among them, Experiment 5, the control group without obstacles, had the longest evacuation time. In this experiment, pedestrians could move freely towards the exit without constraints and quickly formed a high-density area near the exit. During the waiting process, the unfair competition tendency among pedestrians increased, resulting in more collisions between pedestrians and exacerbating congestion. Compared to the other four experiments, this research concludes that obstacles can, to some extent, alleviate congestion and improve evacuation efficiency.

Experiment 2 had the shortest evacuation time, and the congestion near the exit was minimal among all experiments. In Experiment 2, the obstacles divided pedestrians into four orderly queues. Compared with Experiment 1, the pedestrians reduced the process of bypassing the obstacles, and almost only needed lateral movement to reach the exit. This is the main reason why the evacuation time of Experiment 2 was lower than that of Experiment 1. This shows that obstacles have two effects on pedestrians: guidance and hindrance. When the evacuation path is directly connected with the exit, the role of obstacles is mainly reflected in dividing the queue and guiding pedestrians. This condition is more conducive to evacuation.

Although the total width of the passages was the same for Experiment 1 and Experiment 3, the evacuation time of Experiment 3, with only one wide path, was longer than that of Experiment 1, with three narrow paths. In Experiment 3, pedestrians only progressed in an orderly manner before reaching the wide path. Once pedestrians reached the wide path, they immediately transitioned into disordered movement. Pedestrians formed a high-density area after rapidly reaching the exit. During the waiting process, the unfair competition tendency among pedestrians increased, leading to more collisions between pedestrians and exacerbating congestion. In Experiment 1, the three narrow paths were all set to 1.1 m. At this point, the obstacles effectively constrained the formation of queues, thereby reducing interactions between pedestrians from different queues. Therefore, under equal total width conditions, the evacuation efficiency of multiple narrow paths was higher than that of a single wide path.

Experiment 4 increased the area of the obstacle-free zone in front of the exit. Through comparison, it was found that the smaller the area where pedestrians move in a disorderly manner, the shorter the evacuation time of the pedestrians. In Experiment 1, the area of disorderly movement was small, and many pedestrians queued in an orderly manner at paths, which did not increase the congestion near the exit. This explains why Experiment 1 had a shorter evacuation time compared to Experiment 4. The indoor layout should give full play to the constraint of obstacles on pedestrians and reduce the area of the disorderly area near the exit.

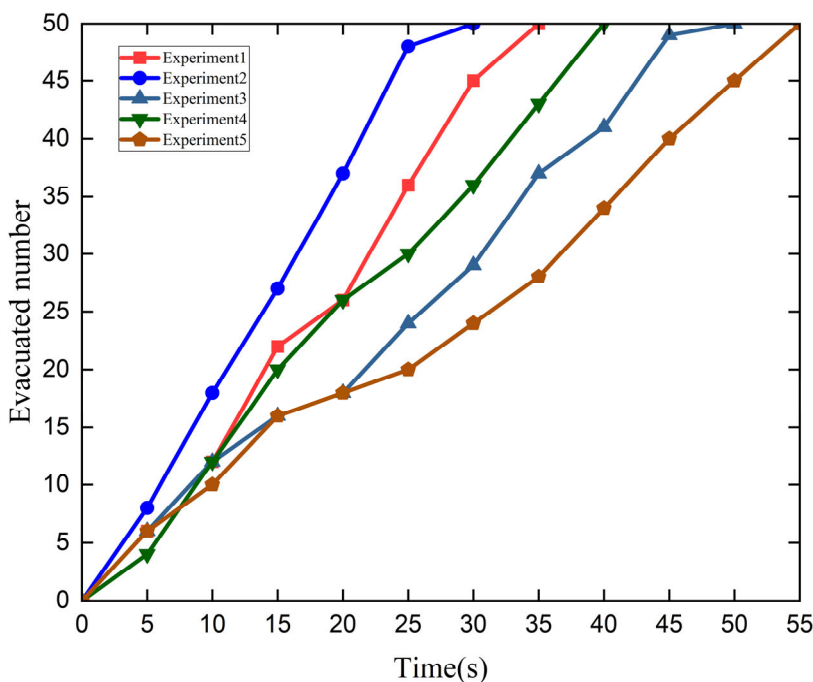


Figure 9. The relationship between the number of evacuees and time in each experiment.

### 6. Conclusions

The MSFM introduces unfair competition behavior based on the SFM, analyzing the causes and psychological tendencies of this behavior. This model considers the impact of the gap between pedestrians’ actual and maximum achievable speed, pedestrian effective radius, and queue length on desired speed. By increasing the desired speed, more collisions among pedestrians are achieved. The MSFM also introduces the feature of variable pedestrian effective radius. The effective radius of pedestrians dynamically changes based on the surrounding crowd density and queue time. The simulation results indicate that the model can better simulate pedestrian evacuation in hazardous situations.

By adjusting the layout of obstacles, this research analyzes the impact of the relative positioning of obstacles to the exit, the number of evacuation paths, and the size of obstacle-free areas in front of the exit. When obstacles play a role in guiding or reducing the interaction of pedestrians in different queues, it has a positive impact on improving evacuation efficiency. When obstacles hinder pedestrians, the evacuation efficiency is reduced to a certain extent. Based on the above conclusions, the following suggestions are put forward:

- Under the premise of meeting functional requirements, indoor installation should avoid centralized placement of fixed facilities as much as possible. It is suggested to use fixed facilities to divide the room into multiple regular and independent areas, thereby forming multiple narrow evacuation paths. Each area should have independent evacuation paths leading to the exit to avoid congestion and confusion caused by pedestrian interaction in different queues.
- The layout of fixed facilities should consider that the evacuation path formed by them can lead directly to the exit. Even if the visibility is low in the fire environment, pedestrians can reach the exit quickly and smoothly by walking on the edge of the fixed facilities.
- Managers should regularly conduct fire safety education to increase pedestrians' confidence in surviving during hazardous events. This helps to reduce tendencies towards unfair competition from a psychological perspective.

This research discusses the impact of fixed obstacles on pedestrian emergency evacuation. However, during a fire incident, flammable or easily collapsible objects may randomly appear in evacuation pathways. The effects of these randomly appearing or non-fixed obstacles on pedestrian evacuation need to be further discussed in future research.

**Author Contributions:** Conceptualization, S.L.; methodology, S.L.; software, X.L. and B.P.; validation, X.L. and B.P.; formal analysis, S.L.; investigation, X.L. and B.P.; data curation, S.L.; writing—original draft, S.L.; writing—review and editing, S.L.; visualization, S.L.; supervision, C.L.; project administration, C.L.; funding acquisition, C.L. All authors have read and agreed to the published version of the manuscript.

**Funding:** This research was funded by the Shanghai Social Science Foundation (No. 2023BSH003, 22Z350204369 and 2022BSH005); the Shanghai Scientific Research Foundation (No. 23DZ1202900, 23DZ1203200, 23DZ1202400, 22DZ1203200, 21Z510203259 and 21DZ1200800); the Scientific Research Fund from Shanghai Municipal Engineering Design Institute (Group) Co., Ltd. (No. K2015K017); and the Laboratory of Advanced Public Transportation Science Program (No. 2020-APTS-04).

**Institutional Review Board Statement:** Not applicable.

**Informed Consent Statement:** Not applicable.

**Data Availability Statement:** The original contribution of the research has been included in the article, and video data can be found in Ref. [49]. Further inquiries can be directed to the corresponding author.

**Conflicts of Interest:** The authors declare no conflicts of interest.

## Appendix A

The following table contains the pedestrian ID, frame, rotation angle, actual effective radius, and effective radius calculated with different  $\beta$  for 14 cases of pedestrians with noticeable body rotation or contraction behaviors. The pedestrian IDs correspond to those in Ref. [49].

ID	Flame	Rotation Angle (°)	Effective Radius (Real)	Effective Radius ( $\beta = 0.25$ )	Effective Radius ( $\beta = 0.5$ )	Effective Radius ( $\beta = 0.75$ )	Effective Radius ( $\beta = 1$ )
1	158	30	0.2341	0.2274	0.2286	0.2291	0.2291
6	87	40	0.2252	0.2276	0.2293	0.2303	0.2308
7	252	30	0.2341	0.2270	0.2276	0.2275	0.2271
11	585	34.2	0.2304	0.2267	0.2269	0.2265	0.2261
17	69	-	0.2250	0.2279	0.2304	0.2324	0.2341
17	346	69	0.2048	0.2269	0.2273	0.2271	0.2267
20	60	37	0.2279	0.2284	0.2321	0.2361	0.2400
22	39	47	0.2192	0.2281	0.2311	0.2339	0.2364
30	315	44.8	0.2210	0.2270	0.2277	0.2276	0.2273
58	56	24.9	0.2384	0.2280	0.2307	0.2331	0.2351
66	56	29.6	0.2344	0.2281	0.2309	0.2336	0.2359
66	235	25.8	0.2377	0.2272	0.2281	0.2283	0.2281
66	339	41.5	0.2239	0.2268	0.2272	0.2269	0.2265
75	28	19.2	0.2427	0.2284	0.2326	0.2371	0.2415

## References

- Ma, Y.Y.; Zhang, Z.C.; Zhang, W.K.; Lee, E.W.; Shi, M. Development of a time pressure-based model for the simulation of an evacuation in a fire emergency. *J. Build. Eng.* **2024**, *87*, 109069.
- García, A.; Hernández-Delfin, D.; Lee, D.-J.; Ellero, M. Limited visual range in the Social Force Model: Effects on macroscopic and microscopic dynamics. *Phys. A Stat. Mech. Its Appl.* **2023**, *612*, 128461.
- Liu, J.; Zhang, H.; Ding, N.; Li, Y. A modified social force model for sudden attack evacuation based on Yerkes–Dodson law and the tendency toward low risk areas. *Phys. A Stat. Mech. Its Appl.* **2024**, *633*, 129403.
- Sticco, I.M.; Cornes, F.E.; Frank, G.A.; Dorso, C.O. Beyond the faster-is-slower effect. *Phys. Rev. E* **2017**, *96*, 052303.
- Ghani, N.M.; Selamat, H.; Khamis, N.; Ghazalli, S.A. Crowd modelling validation for modified social force model. *Int. J. Integr. Eng.* **2020**, *12*, 10–18.
- Sticco, I.M.; Frank, G.A.; Cornes, F.E.; Dorso, C.O. A re-examination of the role of friction in the original Social Force Model. *Saf. Sci.* **2020**, *121*, 42–53.
- Rangel-Galván, M.; Ballinas-Hernández, A.L.; Rangel-Galván, V. Thermo-inspired model of self-propelled hard disk agents for heterogeneous bidirectional pedestrian flow. *Phys. A Stat. Mech. Its Appl.* **2024**, *635*, 129500.
- Song, Y.; Hu, X.; Shen, L.; Weng, W. Modeling domino effect along the queue using an improved social force model. *Phys. A Stat. Mech. Its Appl.* **2023**, *625*, 129008.
- Üsten, E.; Lügering, H.; Sieben, A. Pushing and non-pushing forward motion in crowds: A systematic psychological observation method for rating individual behavior in pedestrian dynamics. *Collect. Dyn.* **2022**, *7*, 1–16.
- Tian, H.-H.; Wei, Y.-F.; Dong, L.-Y.; Xue, Y.; Zheng, R.-S. Resolution of conflicts in cellular automaton evacuation model with the game-theory. *Phys. A Stat. Mech. Its Appl.* **2018**, *503*, 991–1006.
- Helbing, D.; Buzna, L.; Johansson, A.; Werner, T. Self-organized pedestrian crowd dynamics: Experiments, simulations, and design solutions. *Transp. Sci.* **2005**, *39*, 1–24.
- Shi, M.; Lee, E.W.M.; Ma, Y. A dynamic impatience-determined cellular automata model for evacuation dynamics. *Simul. Model. Pract. Theory* **2019**, *94*, 367–378.
- Fu, L.; Fang, J.; Cao, S.; Lo, S. A cellular automaton model for exit selection behavior simulation during evacuation processes. *Procedia Eng.* **2018**, *211*, 169–175.
- Hu, X.; Chen, T.; Deng, K.; Wang, G. Effects of aggressiveness on pedestrian room evacuation using extended cellular automata model. *Phys. A Stat. Mech. Its Appl.* **2023**, *619*, 128731.
- Guan, J.; Wang, K. Towards pedestrian room evacuation with a spatial game. *Appl. Math. Comput.* **2019**, *347*, 492–501.
- von Schantz, A.; Ehtamo, H. Pushing and overtaking others in a spatial game of exit congestion. *Phys. A Stat. Mech. Its Appl.* **2019**, *527*, 121151.
- Ma, L.; Chen, B.; Chen, L.; Xu, X.; Liu, S.; Liu, X. Data driven analysis of the desired speed in ordinary differential equation based pedestrian simulation models. *Phys. A Stat. Mech. Its Appl.* **2022**, *608*, 128241.
- Yuan, Z.; Jia, H.; Zhang, L.; Bian, L. A social force evacuation model considering the effect of emergency signs. *Simulation* **2018**, *94*, 723–737.
- Yang, X.; Yang, X.; Pan, F.; Kang, Y.; Zhang, J. The effect of passenger attributes on alighting and boarding efficiency based on social force model. *Phys. A Stat. Mech. Its Appl.* **2021**, *565*, 125566.
- Helbing, D.; Farkas, I.; Vicsek, T. Simulating dynamical features of escape panic. *Nature* **2000**, *407*, 487–490.

21. Helbing, D.; Farkas, I.J.; Molnar, P.; Vicsek, T. Simulation of pedestrian crowds in normal and evacuation situations. *Peestr. Evacuation Dyn.* **2002**, *21*, 21–58.
22. Fukamachi, M.; Nagatani, T. Sidle effect on pedestrian counter flow. *Phys. A Stat. Mech. Its Appl.* **2007**, *377*, 269–278.
23. Guo, N.; Hu, M.-B.; Jiang, R. Impact of variable body size on pedestrian dynamics by heuristics-based model. *Phys. A Stat. Mech. Its Appl.* **2017**, *465*, 109–114.
24. Jin, C.-J.; Jiang, R.; Yin, J.-L.; Dong, L.-Y.; Li, D. Simulating bi-directional pedestrian flow in a cellular automaton model considering the body-turning behavior. *Phys. A Stat. Mech. Its Appl.* **2017**, *482*, 666–681.
25. Yamamoto, H.; Yanagisawa, D.; Feliciani, C.; Nishinari, K. Body-rotation behavior of pedestrians for collision avoidance in passing and cross flow. *Transp. Res. Part B Methodol.* **2019**, *122*, 486–510.
26. Chraïbi, M.; Seyfried, A.; Schadschneider, A. Generalized centrifugal-force model for pedestrian dynamics. *Phys. Rev. E* **2010**, *82*, 046111.
27. Zheng, X.; Palffy-Muhoray, P. Distance of closest approach of two arbitrary hard ellipses in two dimensions. *Phys. Rev. E* **2007**, *75*, 061709.
28. Chen, H.; Zhang, X. Path planning for intelligent vehicle collision avoidance of dynamic pedestrian using Att-LSTM, MSFM, and MPC at unsignalized crosswalk. *IEEE Trans. Ind. Electron.* **2021**, *69*, 4285–4295.
29. Fu, L.; Qin, H.; He, Y.; Shi, Y. Application of the social force modelling method to evacuation dynamics involving pedestrians with disabilities. *Appl. Math. Comput.* **2024**, *460*, 128297.
30. Zhao, Y.; Lu, T.; Su, W.; Wu, P.; Fu, L.; Li, M. Quantitative measurement of social repulsive force in pedestrian movements based on physiological responses. *Transp. Res. Part B Methodol.* **2019**, *130*, 1–20.
31. Hu, X.; Chen, T.; Song, Y. Anticipation dynamics of pedestrians based on the elliptical social force model. *Chaos Interdiscip. J. Nonlinear Sci.* **2023**, *33*, 073102.
32. Su, B.; Andelfinger, P.; Kwak, J.; Eckhoff, D.; Cornet, H.; Marinkovic, G.; Cai, W.; Knoll, A. A passenger model for simulating boarding and alighting in spatially confined transportation scenarios. *J. Comput. Sci.* **2020**, *45*, 101173.
33. Ronayne, D.; Sgroi, D.; Tuckwell, A. Evaluating the sunk cost effect. *J. Econ. Behav. Organ.* **2021**, *186*, 318–327.
34. Ohlert, C.R.; Weißenberger, B.E. Debiasing escalation of commitment: The effectiveness of decision aids to enhance de-escalation. *J. Manag. Control* **2020**, *30*, 405–438.
35. Lu, L.; Ji, J.; Zhai, C.; Wang, S.; Zhang, Z.; Yang, T. Research on the Influence of Narrow and Long Obstacles with Regular Configuration on Crowd Evacuation Efficiency Based on Tri-14 Model with an Example of Supermarket. *Fire* **2022**, *5*, 164.
36. Chinese Ministry of Housing and Urban-Rural Development. *Code for Fire Protection in Building Design, GB 55037-2022*; China Planning Press: Beijing, China, 2022; pp. 33–34.
37. Lin, P.; Gao, D.L.; Wang, G.Y.; Wu, F.Y.; Ma, J.; Si, Y.L.; Ran, T. The Impact of an Obstacle on Competitive Evacuation Through a Bottleneck. *Fire Technol.* **2019**, *55*, 1967–1981.
38. Li, J.; Wang, J.; Xu, S.; Feng, J.; Li, J.; Wang, Z.; Wang, Y. The effect of geometric layout of exit on escape mechanism of crowd. *Build. Simul.* **2022**, *15*, 659–668.
39. Jia, X.L.; Murakami, H.; Feliciani, C.; Yanagisawa, D.; Nishinari, K. Pedestrian lane formation and its influence on egress efficiency in the presence of an obstacle. *Saf. Sci.* **2021**, *144*, 105455.
40. Yu, W.; Johansson, A. Modeling crowd turbulence by many-particle simulations. *Phys. Rev. E—Stat. Nonlinear Soft Matter Phys.* **2007**, *76*, 046105.
41. Helbing, D.; Farkas, I.J.; Vicsek, T. Freezing by heating in a driven mesoscopic system. *Phys. Rev. Lett.* **2000**, *84*, 1240.
42. Yuen, J.; Lee, E. The effect of overtaking behavior on unidirectional pedestrian flow. *Saf. Sci.* **2012**, *50*, 1704–1714.
43. Helbing, D.; Molnar, P. Social force model for pedestrian dynamics. *Phys. Rev. E* **1995**, *51*, 4282.
44. Andrés-Thió, N.; Ras, C.; Bolger, M.; Lemiale, V. A study of the role of forceful behaviour in evacuations via microscopic modelling of evacuation drills. *Saf. Sci.* **2021**, *134*, 105018.
45. Haghani, M.; Sarvi, M.; Shahhoseini, Z. When ‘push’ does not come to ‘shove’: Revisiting ‘faster is slower’ in collective egress of human crowds. *Transp. Res. Part A Policy Pract.* **2019**, *122*, 51–69.
46. Zhang, W.; Zhang, Z.; Ma, Y.; Lee, E.W.M.; Shi, M. Psychological impatience in pedestrian evacuation: Modelling, simulations and experiments. *Phys. A Stat. Mech. Its Appl.* **2024**, *635*, 129472.
47. You, L.; Wu, Q.; Wei, J.; Hu, J.; Wang, J.; Liang, Y. A study of pedestrian evacuation model of impatient queueing with cellular automata. *Phys. Scr.* **2020**, *95*, 095211.
48. Corbetta, A.; Toschi, F. Physics of human crowds. *Annu. Rev. Condens. Matter Phys.* **2023**, *14*, 311–333.
49. Crowds in Front of Bottlenecks from the Perspective of Physics and Social Psychology. Available online: <http://ped.fz-juelich.de/da/2018crowdqueue> (accessed on 3 January 2018).
50. Cornes, F.E.; Frank, G.A.; Dorso, C.O. Microscopic dynamics of the evacuation phenomena in the context of the Social Force Model. *Phys. A-Stat. Mech. Its Appl.* **2021**, *568*, 125744.

**Disclaimer/Publisher’s Note:** The statements, opinions and data contained in all publications are solely those of the individual author(s) and contributor(s) and not of MDPI and/or the editor(s). MDPI and/or the editor(s) disclaim responsibility for any injury to people or property resulting from any ideas, methods, instructions or products referred to in the content.